

Rashba effect within the space-charge layer of a semiconductor

This content has been downloaded from IOPscience. Please scroll down to see the full text.

2014 New J. Phys. 16 045003

(<http://iopscience.iop.org/1367-2630/16/4/045003>)

View [the table of contents for this issue](#), or go to the [journal homepage](#) for more

Download details:

IP Address: 140.114.80.57

This content was downloaded on 07/04/2014 at 04:44

Please note that [terms and conditions apply](#).

Rashba effect within the space–charge layer of a semiconductor

Chung-Huang Lin¹, Tay-Rong Chang¹, Ro-Ya Liu^{1,2}, Cheng-Maw Cheng²,
Ku-Ding Tsuei^{2,1}, H -T Jeng¹, Chung-Yu Mou¹, Iwao Matsuda³ and
S -J Tang^{1,2}

¹Department of Physics, National Tsing Hua University, Hsinchu, Taiwan 30013, Republic of China

²National Synchrotron Radiation Research Center (NSRRC), Hsinchu, Taiwan 30076, Republic of China

³Institute for Solid State Physics, University of Tokyo, 5-1-5 Kashiwanoha, Kashiwa, Chiba 277-8581, Japan

E-mail: sjtang@phys.nthu.edu.tw

Received 16 October 2013, revised 14 January 2014

Accepted for publication 11 February 2014

Published 4 April 2014

New Journal of Physics **16** (2014) 045003

doi:[10.1088/1367-2630/16/4/045003](https://doi.org/10.1088/1367-2630/16/4/045003)

Abstract

The observed heavy-hole, light-hole and split-off band edges of a semiconductor are the well known consequence of two physical processes: atomic spin–orbital interaction and solid-state band–band anticrossing. In this work, we examined the four band-edge-like bands in great detail within the Ge space–charge layer with either Pb/Ge(111)- $\sqrt{3} \times \sqrt{3}$ R30° or a 2 ML Pb film on Ge(111). Our results reveal that the conventional picture of band edges for a semiconductor is actually crude. In addition, momentum-dependent Rashba splitting effect can be included to explain the observed non-split-off band, indicating the Rashba effect as an intrinsic property near a semiconductor surface.

Keywords: semiconductor band edges, space–charge layer, Rashba effect



Content from this work may be used under the terms of the [Creative Commons Attribution 3.0 licence](https://creativecommons.org/licenses/by/3.0/). Any further distribution of this work must maintain attribution to the author(s) and the title of the work, journal citation and DOI.

1. Introduction

Spin-orbital interaction (SOI) enables the production and manipulation of spin-polarized electrons mainly by an electric field, as the electric field acts on a moving charge carrier as an effective magnetic field [1]. Moreover, at a surface or interface, the inversion asymmetric potential further lifts the spin degeneracy of two-dimensional (2D) electronic bands—the so-called Rashba effect [2]. Such an inversion asymmetric potential was originally considered to be along the surface normal as observed from pure metal surfaces [3–5]. Ast *et al* then found that the in-plane potential gradient also produced a large Rashba spin splitting, as found in surface alloys such as Bi/Ag(111) [6] and Bi/Si(111) [7]. Bychkov–Rashba SOI was initially proposed for a 2D electron gas of semiconductor heterostructures [2]. Spintronics are more significant industrially and scientifically in semiconductors than in metal systems because several semiconductor-related techniques are applicable to engineer device function [8, 9], and the spin–Hall effect in semiconductors with strong spin–orbital coupling is well known [10]. One question nevertheless remains: would Rashba spin splitting exist on or near a pure semiconductor surface? For a highly doped semiconductor, the density of donor or acceptor ions accumulated on the surface can be considered to be constant over the space-charge layer (SCL); according to Poisson’s equation, the resulting potential gradient, or electric field, is a linear function of the depth perpendicular to the surface with the slope proportional to the density of the donor (acceptor) ions [11]. It is therefore likely that intrinsic Ge energy bands within this SCL would be subject to the Rashba effect, and hence exhibit momentum-dependent spin splitting. All preceding work on the Rashba effect of semiconductor surfaces has, however, incorporated heavy-metal atoms thereon [7, 12–14]; the focus was on the localized surface states within the ad-atom or alloy layer, but Ohtsubo *et al* [15] found from Bi/Ge(111)- $\sqrt{3} \times \sqrt{3}$ R30° that surface-state and surface-resonance bands around the surface zone center exhibit a characteristic spin structure, which is induced by a SOI of a lighter element, Ge, with a negligible contribution from a heavier one, Bi. A similar argument was reached with their further attempt on a Ge(111) surface with a light atom, Br, of 1 ML adsorbed [16]. Their reasoning was based on the simulating result of first-principles calculation, but a real physical mechanism is lacking. Ge is a semiconductor with a SOI induced gap ~ 0.29 eV at the zone center [17]. In this work, we reexamined the resonance-band structures observed in either a Pb/Ge(111)- $\sqrt{3} \times \sqrt{3}$ R30° surface or a 2 ML Pb film on Ge(111), and sought to use an inherent model for the formation of Ge band edges with Rashba splitting assumed to realize and to justify the Rashba effect within the SCL.

2. Methods

2.1. Experimental details

The photoemission measurements were performed with photons of energy 21.2 eV from a He lamp and synchrotron radiation from beamline 21B1-U9 at the National Synchrotron Radiation Research Center in Taiwan. A highly doped *n*-type Ge(111) wafer, $10^{17} - 10^{18}$ cm⁻³, was used. The cleaning procedure for a Ge(111)-c(2 × 8) surface is described elsewhere [18]. To form the Pb/Ge(111)- $\sqrt{3} \times \sqrt{3}$ R30° structure, we deposited ~ 3 ML of the Pb film; the substrate was subsequently annealed from RT to 400 °C. The Pb/Ge(111)- $\sqrt{3} \times \sqrt{3}$ R30° structure thus

obtained is the β phase [19]. An overlayer uniform Pb film was formed on depositing Pb onto the Pb/Ge(111)- $\sqrt{3} \times \sqrt{3}$ R30° structure kept at -150°C . The film thickness was determined from a discrete evolution of the quantum-well states [20].

2.2. Theoretical details

Our first-principles calculations are based on the generalized gradient approximation [21], using the full-potential projected augmented-wave method [22] as implemented in the VASP package [23]. The lattice structure of bulk Ge was optimized with a $13 \times 13 \times 7$ Monkhorst-Pack k -point mesh over the Brillouin zone with cutoff energy of 500 eV. The Ge (111)- 1×1 unreconstructed surface was simulated by a 18-layer Ge slab terminated by a hydrogen layer on the backside. The vacuum thickness was larger than 15 Å, satisfactorily separating the slabs. The self-consistent calculations were performed on $13 \times 13 \times 1$ k -point mesh over the 2D irreducible Brillouin zone. The spin-orbital coupling was included in the band-structure calculations.

3. Results and discussions

3.1. Comparison between data and calculation

Figures 1(a) and (b) show the gray scale of 2D photoemission spectra of the energy-band dispersions for Pb/Ge(111)- $\sqrt{3} \times \sqrt{3}$ R30° surface and a 2 ML Pb film on Ge(111), respectively, in the symmetry direction $\bar{K} - \bar{\Gamma} - \bar{K}$ in terms of a Ge(111) surface Brillouin zone. Three bands resembling heavy-hole(HH), light-hole(LH) and split-off(SO) band edges of Ge are observed in both spectra. On inspecting those bands and comparing them with the calculated bulk Ge band edges (yellow dashed curves in figures 1(c), (d)) in the symmetry direction $K - \Gamma - K$ (parallel to $\bar{K} - \bar{\Gamma} - \bar{K}$), one finds significant differences. First, there exists an extra non-split-off(NSO) band (blue dotted curve), coinciding with the top of the HH and LH at the zone center and crossing the SOI gap between them. Second, the bands resembling the SO and LH band edges appear broader. Those bands must be resonances localized within the Ge SCL [18] so that they become observable from both a Pb/Ge(111)- $\sqrt{3} \times \sqrt{3}$ R30° surface and a 2 ML Pb film on Ge(111), which have disparate lattice structures [18, 20]. According to preceding work [18], the HH-, LH-, and SO-like resonance bands are caused by the coupling between surface states (quantum-well states) and Ge band edges within the SCL, and the NSO-like band is a surface resonance within the Ge gap induced by SOI, but its origin was not addressed. Figure 2 shows the dependence of those band-edge-like resonance bands on photon energies at 21.2, 25, and 30 eV, respectively. As seen, those four bands don't shift or deform except the change in the intensities. Therefore, their 2D nature was further confirmed.

3.2. Band edges of a bulk Ge

To unravel the nature of these resonance bands, one must trace back to the original band edges of a bulk semiconductor. Figure 3(a) shows the prototype model for the formation of three main band edges, HH, LH and SO. The mechanism includes SOI, mostly an atomic effect, and band-band anticrossing interaction (BAI), which is mostly a solid-state effect [24, 25]. Without

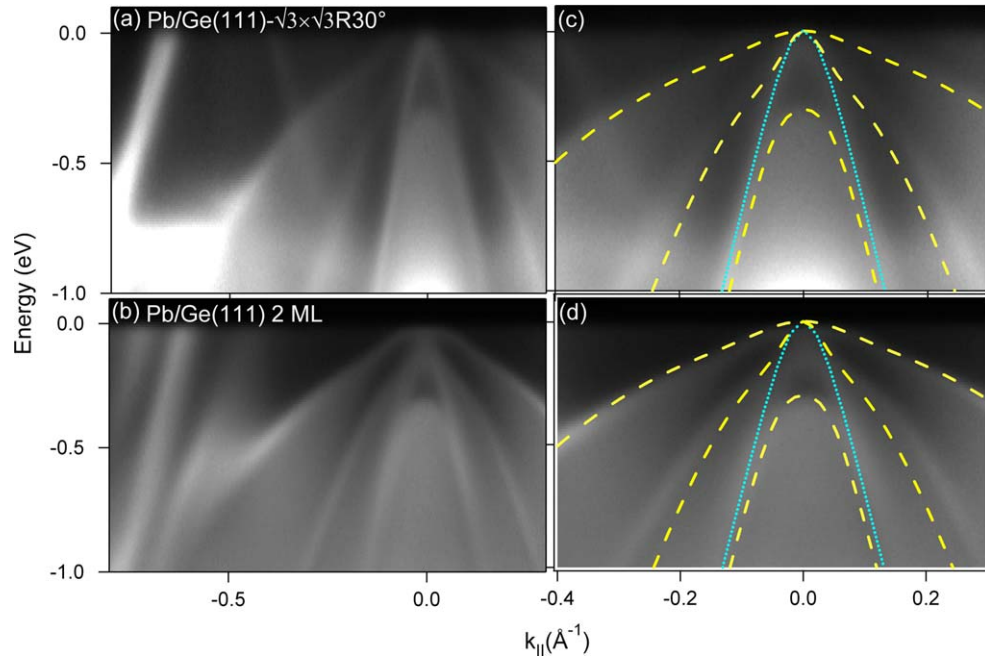


Figure 1. Angle-resolved photoemission data presented as grayscale images as a function of energy and $k_{||}$ for (a) $\text{Pb}/\text{Ge}(111)-\sqrt{3} \times \sqrt{3} R30^\circ$ surface, and (b) 2 ML Pb film on Ge(111), respectively in the symmetry direction $\bar{K}-\bar{\Gamma}-\bar{K}$ in terms of a Ge(111) surface Brillouin zone. (c) and (d) show magnified views of (a) and (b) with calculated Ge bulk band edges superimposed.

SOI, all three band edges are nested at the zone center and are approximately parabolic, but with different curvatures. Due to SOI, the middle band shifts downward by an energy Δ . The shifted middle band then interacts with the bottom band (indicated by the arrows), resulting in an anticrossing gap and consequently the so-called LH and SO band edges. However the formation of HH, which has distinct shape from the top band, is not account for in this crude model. In addition the repulsive anticrossing interaction could make the energy difference between LH and SO band edges at the zone center further larger than Δ . Figure 3(b) displays the subbands pertaining to HH (green), LH (blue) and SO (red) on the left-hand side and their corresponding precursors without interactions on the right hand side, superimposed onto the 2D photoemission data of 2 ML Pb on Ge(111). The yellow dashed curves denote the band edges, the same as those in figures 1 and 2, derived from the bulk band dispersions $\text{K}-\bar{\Gamma}-\text{K}$. As seen, part of HH subbands aggregate densely onto the band edge of LH, causing the delusion of broadening of LH band edge (pink dashed-dot curve). This possibly explains the deviation between LH-like resonance band and LH band edge observed in figures 1 and 2. Such effect is also observed from the band edges without interaction (the right-hand side of figure 3(b)) however with less relevance. The first-principles calculated orbital symmetry of HH, LH and SO as well as their counterparts without interactions are exhibited in figure 3(c). The electron states of HH, LH and SO are mainly p_z , p_y and p_x type, manifesting themselves for the atomic spin-orbital splitting. However, one can see the orbital symmetry of SO band edge turns more s -like when being away from the zone center. In addition, HH, LH and SO band edges have slight mixture with p_y , p_x , and s -type symmetry, respectively, near the zone center, which are not observed for their

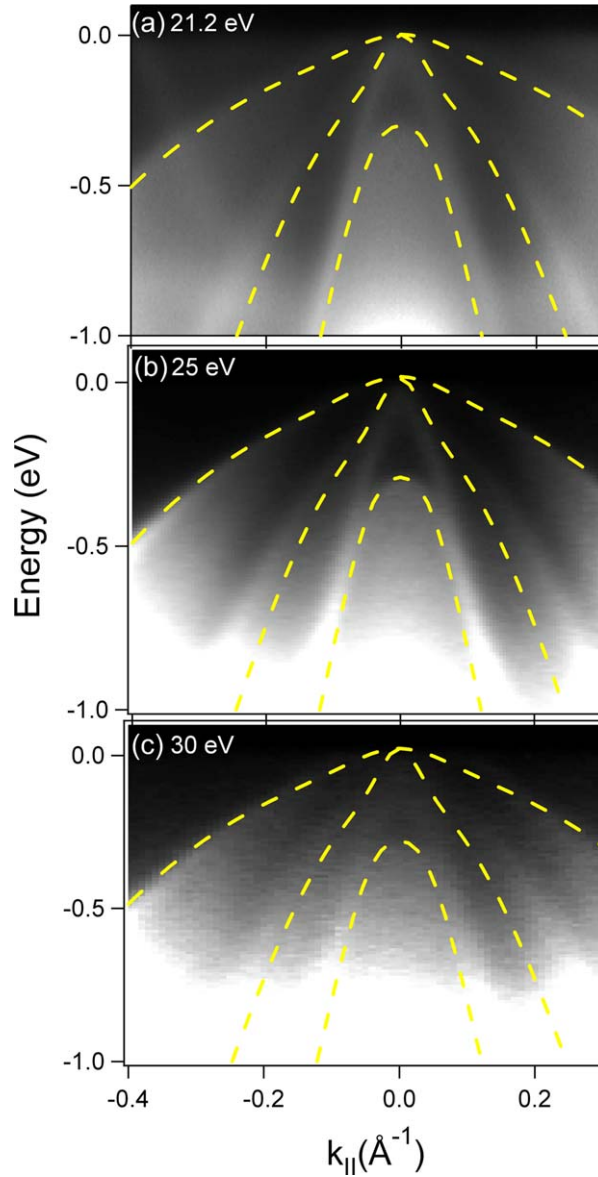


Figure 2. The photon energy dependence of four band-edge-like bands observed in Pb/Ge(111)- $\sqrt{3} \times \sqrt{3}$ R30° surface. The yellow dashed curves are the bulk band edges as those in figure 1.

counterparts without interaction. Hence, this confirms the band-band interactions among them for the formation of Ge band edges.

3.3. Band edges of a Ge space charge layer

Up to here, the deviation on the LH band edge between the calculation and data is likely resolved in the context of Ge bulk. Yet the existence of extra NSO band and the broadening of SO-like resonance band should be further investigated in light of SCL, within which electronic bands are inherently 2D. Due to the extra potential induced by charge accumulation on the semiconductor surfaces, the energy position of the bulk band edges in SCL shifts upward or

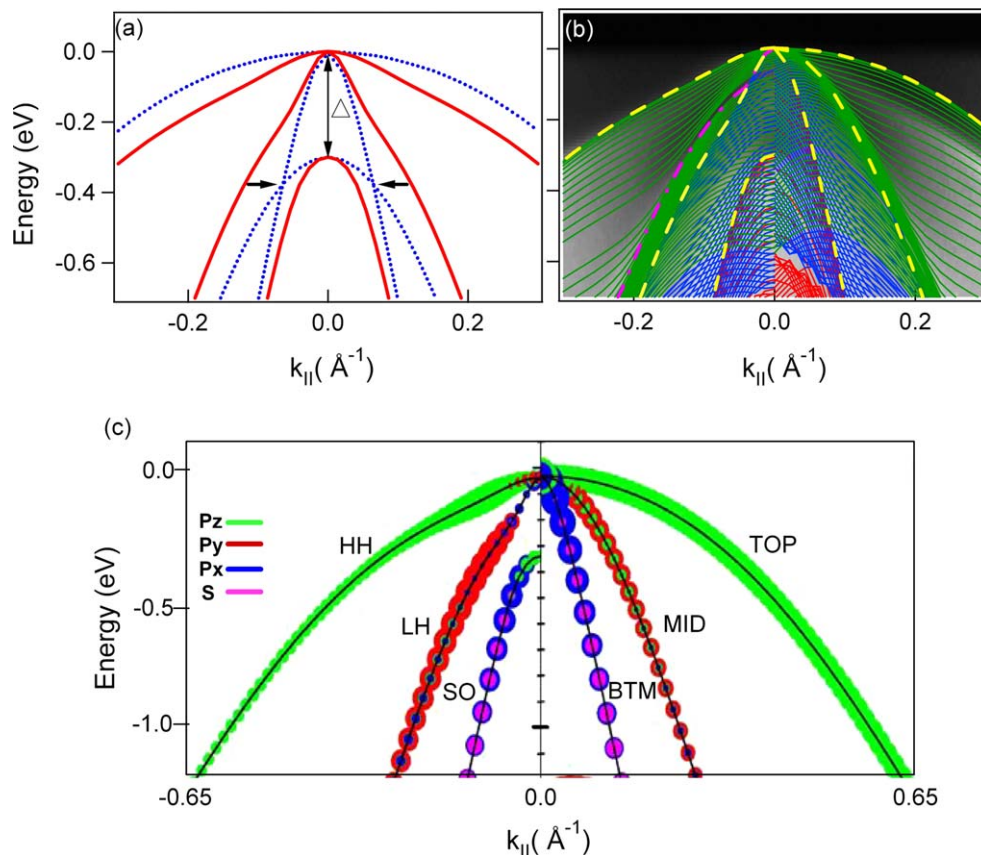


Figure 3. (a) The three band edges of a bulk Ge before and after the interactions. (b) The subbands pertaining to HH, LH and SO band edges before (right-hand side) and after (left-hand side) interactions in the directions parallel to $\vec{K}-\vec{\Gamma}-\vec{K}$. (c) The orbital symmetries of HH, LH and SO band edges before (right-hand side) and after (left-hand side) interactions in the direction $\vec{K}-\vec{\Gamma}-\vec{K}$, derived by first-principle calculations.

downward as a function of the position in the direction normal to the surface—so-called band bending. Moreover, the confinement effect of the SCL, which is more evident in the highly doped condition, yields discrete or quantized subbands of band edges [24]. A further effect within the SCL, which might have been overlooked, is the Rashba effect. Figure 4(a) shows the precursors of three band edges, top, middle and bottom, of the Ge SCL without SOI; their tops coincide at the zone center, which is arbitrarily set at the Fermi level. Subsequently, as shown in figure 4(b), the middle band shifts down by Δ from the top band because of SOI. At this point, if the Rashba effect enters, those band edges would spin-split in the $\pm k_{||}$ direction following time-reversal symmetry. In turn, this condition produces a great change in the consequence of the following anticrossing interaction between the middle and bottom band edges because of the spin-selection rule for the interaction [26]. The spin splitting of the bottom band edge is considered to be negligible as it has quite large s -type symmetry with increasing $k_{||}$ (figure 3(c)), resulting in a zero value of the matrix element for SOI. As shown in figure 4(c), the resulting HH, LH and SO bands are spin-polarized (red for spin up and blue for spin down); the inner parts of the spin-polarized LH bands constitute what appears to be the NSO band observed within the SCL of Ge. This is understandable since the spin-selection rule allows one of the

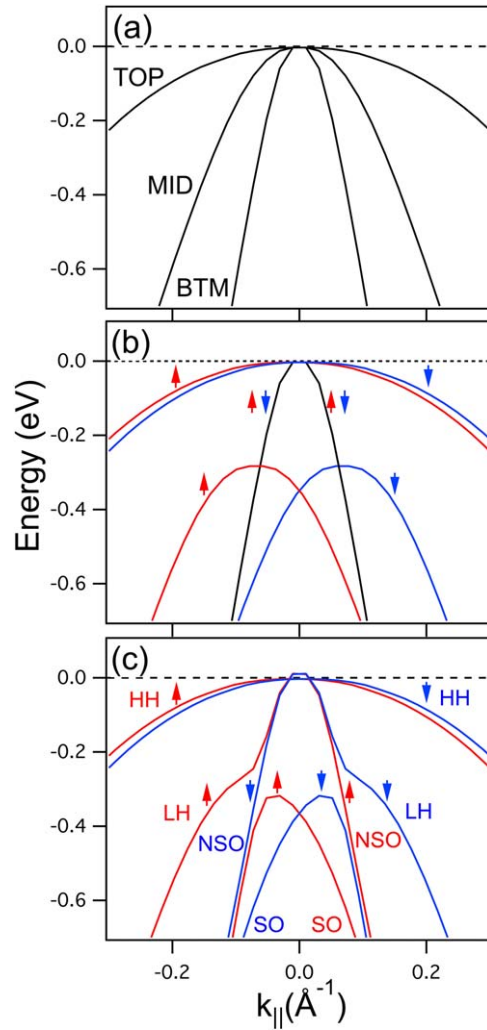


Figure 4. Proposed model for the formation of observed Ge band edges within SCL. Dark, blue and red colors indicate spin-degenerate, spin-up and spin-down band edges, respectively.

degenerate bottom bands, equivalent to NSO band, to pass the anticrossing gap. The spin splitting of SO bands then leads to the observed broadening. Through the repulsive BAI, the top of the LH would slightly overshoot that of the precursor of the HH band, causing its deformation after the interaction.

3.4. Model fitting

To make a full simulation, all subbands on behalf of the band edges⁴, middle and bottom, must be taken into account to undergo these three effects, namely SOI, BAI and the Rashba effect, which are summarized in terms of the Hamiltonian matrix as

⁴ The top band was considered to be degenerate and non-interacting in our simulation because our focus was on the resulting LH, SO and NSO band edges.

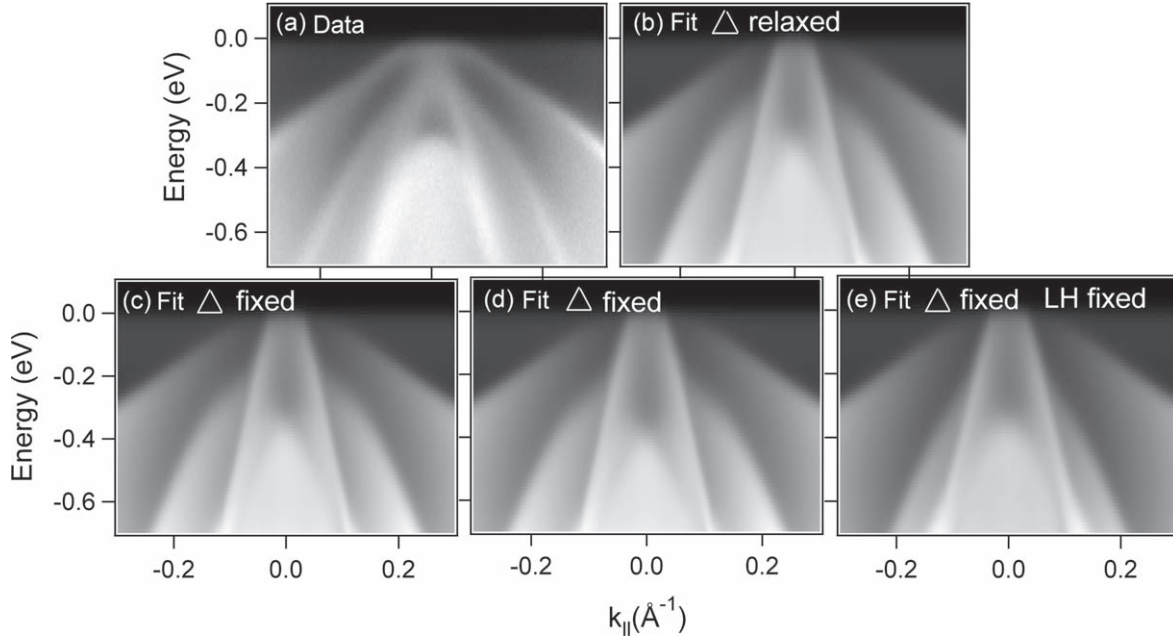


Figure 5. (a) The 2D photoemission data for 2 ML Pb film on Ge(111) in the symmetry direction $\bar{K} - \bar{\Gamma} - \bar{K}$. (b) The resulting 2D fitting result with spin-orbital splitting value Δ relaxed. (c) The resulting 2D fitting result with Δ fixed to be 0.27 eV. (d) The resulting 2D fitting result with Δ fixed to be 0.29 eV. (e) The resulting 2D fitting result with Δ fixed to be 0.29 eV and spin-polarized LH bands fixed as the bulk counterpart.

$$\begin{bmatrix} E_{mid}^i(\uparrow) & 0 & c & 0 \\ 0 & E_{mid}^i(\downarrow) & 0 & c \\ c & 0 & E_{btm}^i(\uparrow) & 0 \\ 0 & c & 0 & E_{btm}^i(\downarrow) \end{bmatrix}, \quad (1)$$

Here c represents the matrix element for the BAI potential, which is assumed to be an overall constant, and arrows denote the spin polarization perpendicular to the momentum direction. The energy eigenvalues of subband i for the middle and bottom band edges before the BAI have forms

$$E_{mid}^i(\uparrow\downarrow) = E_{mid}^i(k_{\parallel} \pm \beta) - \Delta \quad (2)$$

$$E_{btm}^i(\uparrow\downarrow) = E_{btm}^i(k_{\parallel}) \quad (3)$$

in which β and Δ represent respectively the momentum offset by Rashba splitting and the energy shift by atomic SOI. These two quantities are assumed to be constant over all subbands. With the calculated bulk Ge subbands (without SOI considered) for E_{mid}^i and E_{btm}^i and with c and β as fitting parameters, the 2D photoemission spectra of LH-, SO- and NSO-like bands in figure 5(a) from 2 ML Pb film on Ge(111) were then fitted by the spectra function [20, 25]

$$A(k_{\parallel}, E) \propto \sum_{i=1}^5 |\langle \Psi_{\text{Pb}} | V_i | \Psi_{\text{Ge}} \rangle|^2 g_i(k_{\parallel}, E) \quad (4)$$

with the addition of a smooth background function and lifetime and instrumental broadening, where the hybridization matrix element $\langle \Psi_{\text{Pb}} | V_i | \Psi_{\text{Ge}} \rangle$, with $i = 1-5$ for the Ge valence bands, is each taken to be a constant in the thin film limit, k_{\parallel} is the in-plane wave vector, and $g_i(k_{\parallel}, E)$ is the density of states of Ge in 1D form, adopted from the HH band edge and spin-polarized band edges of LH, SO and NSO derived through relations (1), (2) and (3). We sampled 50 k -points distributed uniformly between the bulk Ge symmetry points Γ and L for the onsets of all subbands. The resulting band edges are formed by the summations of a partial contribution from each subband. Nevertheless, a definite fitting result could still not be achieved due to the facts previously revealed through examining the band edges of a bulk Ge; first, the possible larger gap size between the tops of LH and SO bands than the actual spin-orbital splitting value Δ and second, the unreal broadening of the LH band edge due to the partial aggregation of HH subbands. Thus, we carry out the fitting on four different conditions. Figure 5(b) shows the fitting results with Δ value relaxed. Figures 5(c), (d) show the results with Δ value fixed to be 0.26 and 0.29 eV. The fitting goodness in figure 5(b) is the best with the resulting $\Delta = 0.24$ eV, $c = 0.1$ eV and $\beta = 0.06 \text{ \AA}^{-1}$. The fitting goodness in figure 5(d) is apparently worse with much larger gap size ~ 0.38 eV than Δ (0.29 eV). This enlargement of the gap size is, as mentioned before, due to the effect from the repulsive anticrossing interaction. Such result infers that the spin-orbital splitting value Δ within the SCL is substantially smaller than the commonly known value ~ 0.29 eV for a bulk Ge [17]. On the other hand, the adsorbate (Pb atoms) on Ge(111) could also possibly decrease the spin-orbital splitting value of Ge, which was found to be 0.28 eV for Bi/Ge(111)- $\sqrt{3} \times \sqrt{3}$ R30° [15]. In spite of that, the NSO band as well as the broadening of SO-like band is well reproduced in all fitting conditions, confirming the Rashba effects within Ge SCL. The Rashba splitting constants α_R extracted from the figures 5(b)–(d) via the relation $\alpha_R = \frac{\hbar^2 \beta}{m^*}$ (with the effective mass, $0.279 m_e$, extrapolated from the calculated middle band edge before BAI) are 1.35, 1.44, and 1.52 eV \AA , respectively. Figure 5(e) shows the fitting result with both Δ fixed at 0.29 eV and spin-polarized LH band edge fixed as that of bulk Ge depicted by the yellow dashed curve in figure 1. The corresponding Rashba splitting constant then reduces to 0.83 eV \AA simply because the Rashba spin splitting is proportional to the k_{\parallel} range the spin-polarized LH band edges span, as illustrated in figures 4(b), (c). As for the HH band edge, the Rashba splitting within the SCL is expected to be much smaller, and thus not resolved with the limited resolution of our measuring system. The Rashba α_R values of HH (mainly p_z type) and other band edges (mainly p_x or p_y type) can differ largely because of the orbital-symmetry dependence of Rashba splitting [27].

3.5. First-principles calculations of the Ge space charge layer based on a slab model

Following from our model, the observed LH-, SO- and NSO-like bands must be spin-polarized. In order for further confirmation, we therefore performed first-principles calculation for a Ge slab composed of 18 layers with one surface terminated by hydrogen atoms. Figure 6(a) shows the calculated band dispersions in the symmetry direction $\bar{K} - \bar{\Gamma} - \bar{K}$, where the dashed and the solid curves represent the surface states and the resonance states. Certainly, our focus is on

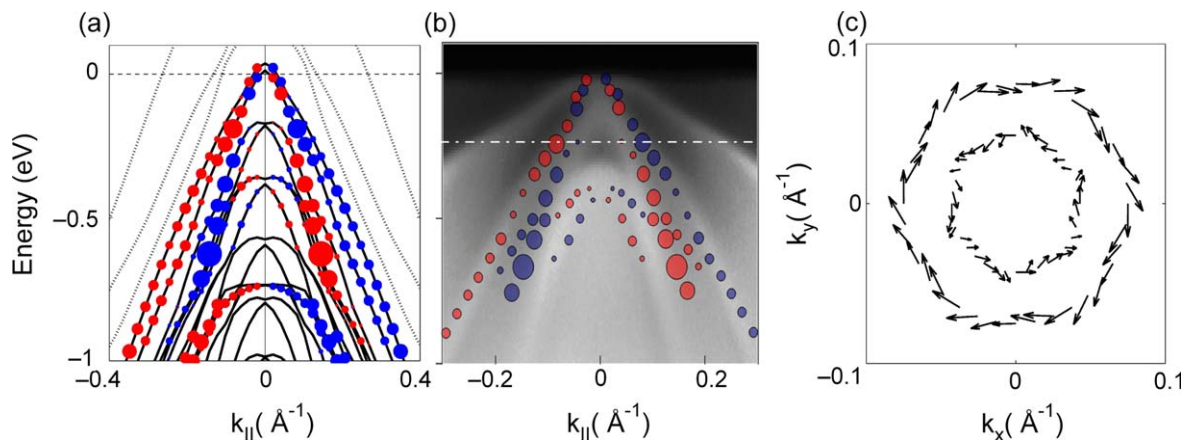


Figure 6. (a) The calculated subband dispersions of a Ge(111) space charge layer in the symmetry direction $\bar{K} - \bar{\Gamma} - \bar{K}$, based on a 18-layer slab model. (b) Superimposition of the calculated subbands most resembling LH- and SO-like bands onto the 2D photoemission data. (c) Spin texture of the electron states of the calculated LH- and NSO-like bands in $k_x k_y$ plane sampled at energy positions indicated by the dash-dotted line in (b).

the latter. The spin polarizations of the electronic states of each subband were denoted by circles with the magnitudes proportional to their sizes and colors indicating the directions; red and blue colors denote the opposite in-plane directions. As seen, the spin polarizations of the subbands follow the time-reversal symmetry with respect to the surface zone center, the essential property of Rashba effects. Moreover, we pick up the calculated subbands most resembling the LH, NSO and SO band edges and superimposed them onto figure 6(b) with the adjustment of energy offset; one can see the resemblance of the spin-direction assignments for NSO and SO bands between figure 4(c) and figure 6(b). The spin textures of the constant energy contours of the calculated subbands resembling the LH, and NSO band edges are further examined at energy position -0.23 eV, indicated by the white dash-dotted line; they exhibit two hexagonal contours with major spin polarizations perpendicular to the momentum direction in $k_x k_y$ plane rotating about the surface zone center in the similar manner to those formed by a typical Rashba splitting. The spin polarizations of the outer (LH) and inner (NSO) contours have opposite directions with their maximums as 50% and 30% of full polarization, respectively. The hexagonal warping shape is due to the fact that the electronic states at -0.3 eV are substantially subjected to the Ge crystal potential. It is very interesting to note that the hexagonal contours corresponding to LH and NSO band edges are 30° rotated to each other. Such behavior was also observed from the spin-splitting constant energy contours derived from the conduction band minimum of the giant bulk Rashba semiconductor BiTeI [28], which possesses trigonal layered structures. We further extrapolate the Rashba splitting value from the calculated spin-polarized subbands matching SO band edge shown in figure 6(b), and the resulting value α_R , 0.81 eV \AA ($\Delta k_{||} = 0.02$ \AA^{-1} , $m^* = 0.192 m_e$), is very close to the value obtained from the fitting in figure 5(e). Due to the fact that actual LH band edge spans narrower than that observed in the data, the actual Rashba constant α_R is more likely within the range 0.8 – 1.5 . Nevertheless, this range of values is larger than values $\alpha_R = 0.2$ and 0.4 eV \AA previously obtained for systems Bi/Ge(111)-R $30^\circ \sqrt{3} \times \sqrt{3}$ [15] and 1 ML Br on Ge(111) [16], respectively, in which the observed

spin splitting was also contributed mainly by Ge. The Rashba splitting in the latter cases were, however, focused on the energy range between -0.2 eV and E_F , in which the splitting derived from our model is also small, as is obvious in figure 4(c). It is worth noting that two surface resonances bands, S and S' , in Bi/Ge(111)- $\sqrt{3} \times \sqrt{3}$ R30° (figure 3(a) of [15]) have opposite spin polarizations as those of LH and NSO bands in our model (figure 4(c)). The larger values that we obtained should thus stand scrutiny.

4. Conclusion

In conclusion, from the deviation between the measured band-edge-like resonance bands of both the Pb/Ge(111)- $\sqrt{3} \times \sqrt{3}$ R30° surface and a 2 ML Pb film on Ge(111), and the corresponding Ge bulk band edges, we demonstrate the existence of the Rashba effect within SCL. Similar band-edge-like resonance bands were also observed about the surface zone center in other systems, such as Ag films on Ge(111) [25], Au/Ge(100)-c(2 × 8) [29], Au/Ge(111)- $\sqrt{3} \times \sqrt{3}$ R30° [30], Bi/Ge(111)- $\sqrt{3} \times \sqrt{3}$ R30° [15] and 1 ML Br on Ge(111) [16], indicating the universal nature of this Rashba effect within SCL. Especially in the case of Au/Ge(111)- $\sqrt{3} \times \sqrt{3}$ R30°, the observed H2, H3, B1 and B2 bands [30] correspond to the HH-, LH-, SO- and NSO-like bands. H2 and H3 were ascribed to surface resonances that overlap with the Ge bulk band projection, and B1 and B2 were considered as bulk bands [30], consistent with our point that these four bands observed are derived from the bulk band edges within the SCL. The Rashba splitting value α_R within Ge SCL is in the range of 0.8–1.5 eV Å based on both the model fitting and first-principles calculated results. Note that in our first-principles calculation, no doping effect is applied to the modeled Ge slab so it implies that the Rashba splitting value we obtained is mainly attributed to the Ge atoms of the SCL undergoing inversion symmetry breaking as a result of its 2D nature. The Rashba splitting value of other 2D semiconductor system from previous studies is in the order of 0.01 eV Å [31]. Some special reason has to be there for the relatively larger values within Ge SCL. According to the preceding theoretical study [32], the spin-orbital splitting in the highest occupied p states in the Ge crystal is 1.5 times larger than that in the Ge atom due to the covalent bonding, which leads to the compression of the valence orbital. We think the relatively larger Rashba splitting value we obtain might have to do with the asymmetry of covalent bonding nature within Ge SCL. Although a more complete and delicate model for the formation of semiconductor band edges is still needed, our demonstration of the Rashba effect delocalized into the SCL of Ge will definitely contribute to the development of semiconductor spintronics near the surface or interface.

Acknowledgments

We thank Koichiro Yaji for helpful discussions. National Science Council of Taiwan (grants NSC 98-2112-M-007-017-MY3 and NSC 102-2112-M-007-009-MY3) provided support. Much of the work was performed at the National Synchrotron Radiation Research Center of Taiwan. CYM, TRC and HTJ are supported by the National Science Council, Taiwan. HTJ also thanks the National Center for High-Performance Computing (NCHC) and the National Center for Theoretical Science (NCTS), Taiwan, for technical support.

References

- [1] Dil J H 2009 *J. Phys: Condens. Matter* **21** 403001
- [2] Rashba E and Tela F T 1960 *Leningrad* **2** 1224
Rashba E and Tela F T 1960 *Sov. Phys.—Solid State* **2** 1109
- [3] LaShell S, McDougall B A and Jensen E 1996 *Phys. Rev. Lett.* **77** 3419
- [4] Nicolay G, Reinert F, Hübner S and Blaha P 2001 *Phys. Rev. B* **65** 033407
- [5] Koroteev Y M, Bihlmayer G, Gayone J E, Chulkov E V, Blügel S, Echenique P M and Hofmann P 2004 *Phys. Rev. Lett.* **93** 046403
- [6] Ast C R, Henk J, Ernst A, Moeschini L, Falub M C, Pacile D, Bruno P, Kern K and Grioni M 2007 *Phys. Rev. Lett.* **98** 186807
- [7] Gierz I, Suzuki T, Frantzeskakis E, Pons S, Ostanin S, Ernst A, Henk J, Grioni M, Kern K and Ast C R 2009 *Phys. Rev. Lett.* **103** 046803
- [8] Sinova J, Culcer D, Niu Q, Sinitsyn N A, Jungwirth T and MacDonald A H 2004 *Phys. Rev. Lett.* **92** 126603
- [9] Morgenstern M, Georgi A, Straßer C, Ast C R, Becker S and Liebmann M 2012 *Physica E* **44** 1795
- [10] Wunderlich J, Kaestner B, Sinova J and Jungwirth T 2005 *Phys. Rev. Lett.* **94** 047204
- [11] Lüth H 1998 *Surfaces and Interfaces of Solid Materials* 3rd edn (Berlin: Springer)
- [12] Höpfner P *et al* 2012 *Phys. Rev. Lett.* **108** 186801
- [13] Yaji K, Ohtsubo Y, Hatta S, Okuyama H, Miyamoto K, Okuda T, Kimura A, Namatame H, Taniguchi M and Aruga T 2010 *Nat. Commun.* **1** 17
- [14] Sakamoto K *et al* 2009 *Phys. Rev. Lett.* **102** 096805
- [15] Ohtsubo Y, Hatta S, Yaji K, Okuyama H, Miyamoto K, Okuda T, Kimura A, Namatame H, Taniguchi M and Aruga T 2010 *Phys. Rev. B* **82** 201307
- [16] Ohtsubo Y, Hatta S, Kawai N, Mori A, Takeichi Y, Yaji K, Okuyama H and Aruga T 2012 *Phys. Rev. B* **86** 165325
- [17] Schmid U, Christensen N E and Cardona M 1990 *Phys. Rev. B* **41** 5919
- [18] Tang S J, Chang T R, Huang C C, Lee C Y, Cheng C M, Tsuei K D, Jeng H T and Mou C Y 2010 *Phys. Rev. B* **81** 245406
- [19] Morikawa H, Matsuda I and Hasegawa S 2008 *Phys. Rev. B* **77** 193310
- [20] Tang S J, Lee C Y, Huang C, Chang T R, Cheng C M, Tsuei K D, Jeng H T, Yeh V and Chiang T C 2011 *Phys. Rev. Lett.* **107** 066802
- [21] Perdew J P, Burke K and Ernzerhof M 1996 *Phys. Rev. Lett.* **77** 3865
- [22] Kresse G and Joubert D 1999 *Phys. Rev. B* **59** 1758
- [23] Kresse G and Furthmüller J 1996 *Comput. Mater. Sci.* **6** 15
- [24] Takeda S N, Higashi N and Daimon H 2005 *Phys. Rev. Lett.* **94** 037401
- [25] Tang S J, Miller T and Chiang T C 2006 *Phys. Rev. Lett.* **96** 036802
- [26] He K, Hirahara T, Okuda T, Hasegawa S, Kakizaki A and Matsuda I 2008 *Phys. Rev. Lett.* **101** 107604
- [27] Zhu Z, Cheng Y and Schwingenschlögl U 2013 *New J. Phys.* **15** 023010
- [28] Ishizaka K *et al* 2011 *Nat. Mater.* **10** 521
- [29] Meyer S, Schäfer Blumenstein J, Höpfner C P, Bostwick A, McChesney J L, Rotenberg E and Claessen R 2011 *Phys. Rev. B* **83** 121411
- [30] Höpfner P *et al* 2011 *Phys. Rev. B* **83** 235435
- [31] Nitta J, Akazaki T, Takayanagi H and Enoki T 1997 *Phys. Rev. Lett.* **78** 1335
- [32] Hybertsen M S and Louie S G 1986 *Phys. Rev. B* **34** 2920